



## Modeling an innovative low-temperature desalination system with integrated cogeneration in a concentrating solar power plant

Johannes Wellmann<sup>a,\*</sup>, Karl Neuhäuser<sup>a</sup>, Frank Behrendt<sup>a</sup>, Mark Lehmann<sup>b</sup>

<sup>a</sup>Zentralinstitut El Gouna, Technische Universität Berlin, Sekr. FH 5-1, Fraunhoferstr. 33-36, 10587 Berlin, Germany, Tel. +49 30 314 75722/28633, +20 65 3561 462; Fax: +49 30 314 78520; email: [Johannes.wellmann@tu-berlin.de](mailto:Johannes.wellmann@tu-berlin.de) (J. Wellmann)

<sup>b</sup>Watersolutions AG, Steinachermattweg 3, 5033 Buchs, Switzerland

Received 31 March 2014; Accepted 16 June 2014

### ABSTRACT

The thermal desalination systems like multi-effect distillation and multi-stage flush have gone through a strong development process to increase energy efficiency and to improve energy recovery. While these improvements have led to lowered energy consumption, different concepts could be necessary to adapt the thermal desalination systems to renewable energy sources. A specially designed low-temperature desalination driven by low-grade waste heat can be used to desalinate seawater and to clean polluted water with a higher conversion ratio than existing systems. The reason for this improvement is a drastically improved heat transfer of this system, using spray systems for evaporation, and condensation. It was tested in a demonstration plant in El Gouna, Egypt, in cogeneration with diesel generators which used 7 MW<sub>th</sub> to desalinate 500 m<sup>3</sup>/d. This paper introduces a model of the low-temperature desalination process, which is derived from experimental data and technical specifications. It required the development of energy, mass, and material balances of the media streams with respect to the measured data from the demonstration plant. The model is implemented using the energy process simulation software “Epsilon Professional” and combined with a 10-MW<sub>th</sub> concentrating solar power (CSP) plant. The results show the cogeneration of 2.2 MW<sub>el</sub> power in the CSP plant and 520 m<sup>3</sup>/d fresh water in the desalination. Furthermore, the output depends on various process parameters like cogeneration fraction, temperature levels, and input salinity, which are analyzed and discussed.

**Keywords:** Thermal desalination; Low temperature; Waste heat; Cogeneration; Concentrating solar power; Hybrid systems, CSP+D

### 1. Introduction

One of the most urgent and serious problems faced in the MENA region today is the scarcity of fresh water [1–3]. Due to population growth, increasing

standards of living, and overexploitation of existing resources, it is likely that industrial desalination will become one of the key technologies in the near future [2]. Fossil fuel-based desalination is still a costly process mainly applied in the oil-rich countries in the Arabian Gulf. Comparing the solar direct normal

\*Corresponding author.

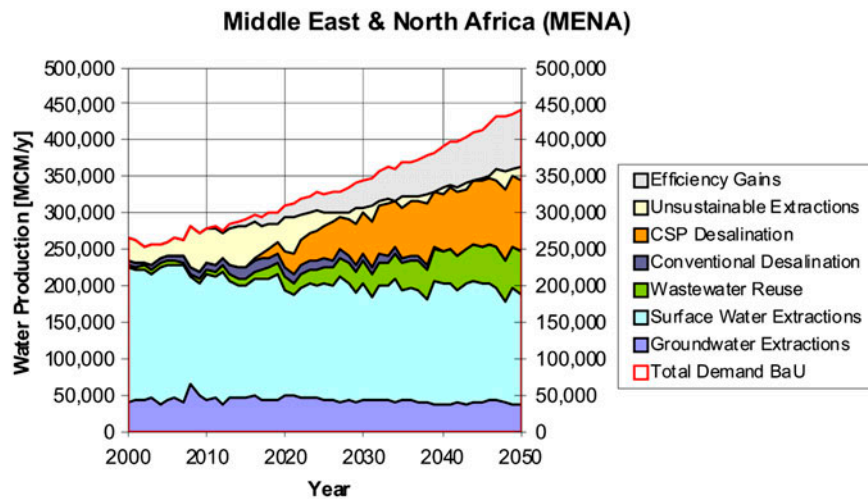


Fig. 1. Water supply within the average climate change scenario for MENA [4].

irradiation of this region and the water supply shows a strong correlation between the potential of concentrating solar power (CSP) plants and water scarcity. A promising solution for increasing the water supply may be the cogeneration of electricity in CSP plants and combined thermal seawater desalination [4]. Within this field, especially low-grade heat-driven desalination technologies have recently attracted much attention, since they have numerous advantages compared to other desalination processes [5]. This technology has just a small effect on the electrical power output of the plant, when the use of cheap waste heat is possible and more reductions in material costs for the solar field can be achieved.

This paper will present an innovative low-temperature thermally driven desalination system, which was demonstrated and tested in El Gouna, Egypt [5]. The model of this system allows the simulation in combination with a CSP plant, which could deliver enough thermal power to generate electricity and fresh water [6].

## 2. Low-temperature desalination

The low-temperature distillation (LTD) process, proposed by Watersolutions AG, Switzerland, is similar to conventional systems like multi-stage flash (MSF) regarding the process flow, but it uses the temperature and pressure dynamics of a multi-effect distillation (MED) system. The system was first built up and tested in El Gouna, Egypt, in combined heat and power configuration with diesel generators in 2009. The LTD uses a special spray system to increase the surface of the

water inside the respective reactor, which causes an efficient and strongly increased specific heat transfer between steam and distillate especially on the condensation side [5]. The measurements of the demonstration plants have shown possible heat transfer rates of more than  $40,000 \text{ W/m}^2\text{K}$  in the reactors [7].

The basic system layout is visualized in Fig. 2. Each stage consists of two connected reactors with an evaporation (1) and condensation (2) side. The system consists of several reactor vessels (evaporation and condensation for each stage), which are flowed through by two major mass flows on each side of the system. This major mass flows (circulation) in the magnitude of  $800 \text{ m}^3/\text{h}$  act as transportation and heat exchange media through the respective heat exchanger (5, seawater and 6, distillate). The reactors are connected by a demister/droplet separator (3) to avoid saltwater in the distillate reactors. Several stages allow more heat efficiency and increase the water production, but increase the investment costs. Those circulating flows require electrical power for pumping not exceeding  $1.5 \text{ kWh/m}^3$  depending on the temperature difference present. Experiments on the demonstration plant have shown that a minimum heat gradient could be approximated to  $1.5 \text{ K}$  between evaporator and condenser for one stage, but the system was designed to run at  $20 \text{ K}$  with two stages at full load.

## 3. Model development

The LTD system is modeled using the software Epsilon Professional V10.0 [8] by adapting the

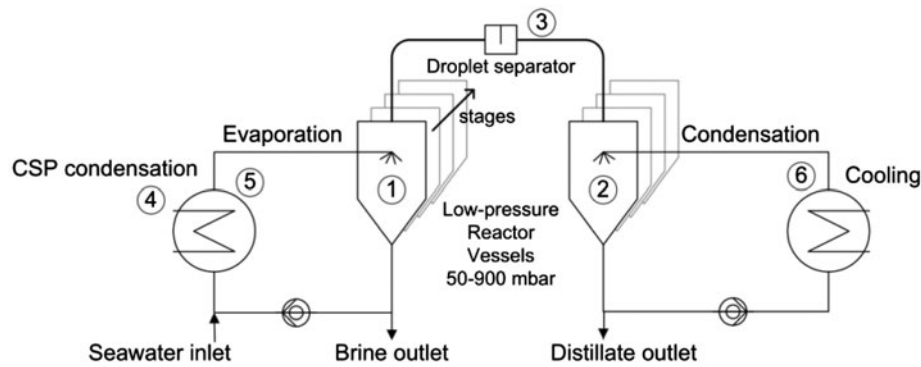


Fig. 2. Process scheme of the LTD system.

scripting kernel module. This simulation environment is suitable to describe the thermodynamic behavior of salt and fresh water as well as the required electric power for pumping. Furthermore, the solar libraries of Epsilon Professional offer a wide set of options to integrate the LTD system in power generating cycles used for CSP plants [8]. This allows a detailed analysis of several system combinations and different parameters.

The media flows are illustrated in Fig. 3. The salt water is heated up in HEX1 and pumped (4) to the first evaporation reactor vessel (E1) in the top of perforated sheet metal trays in order to increase the surface of the water (2). Because of decreased pressure regime in E1, the salt water partially evaporates, while the not-evaporated saltwater mass flow decreases its temperature according to evaporation enthalpy. This leads to a perpetual steam flow, which is assumed to be free of ions and passes through the demister/droplet (3) separator to the condensation reactor vessel C1. The distillate circulation is pumped (7) through similar perforated sheet metal trays inside the condensation reactor to increase its surface. Through cooling down the distillate in HEX3, the generated steam immediately condenses under the perforated steel plates increasing the temperature of the distillate. This process will continue at different temperature/pressure conditions in the following stages: E2–E4 and C2–C4. The heat recovery between evaporation and condensation takes place in HEX2, which further increases the process efficiency.

Describing the temperature correlation between the heat provided in HEX1 with  $T_{HOT\_IN}$  and the cooling in  $T_{COOL\_IN}$  in HEX3, the temperature difference of the whole systems  $\Delta T_{System}$  defines to

$$\Delta T_{System} = T_{Hot\_in} - T_{Cool\_in}$$

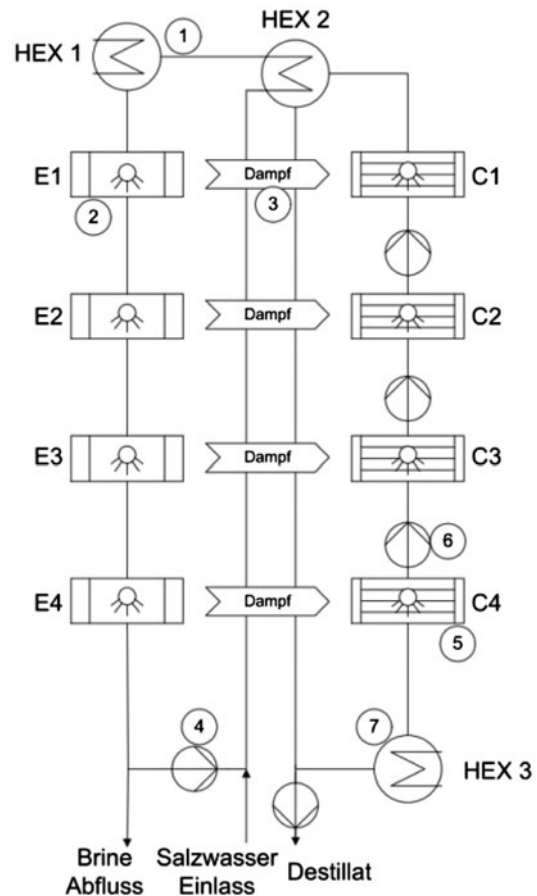


Fig. 3. Saltwater and distillate flows.

According to the specification of the manufacturer, it is required that  $\Delta T_{System}$  should be designed to minimum 10 K for each stage. The temperature difference in the single evaporation or condensation reactor vessels should be  $\Delta T_{Reactor}$ , respectively. The evaporation

and condensation in each stage can be written as  $\Delta T_{\text{Stage}}$  depending on  $i$  stages:

$$\Delta T_{\text{Stage}} = \frac{\Delta T_{\text{System}} - \Delta T_{\text{Reactor}}}{i + 1}$$

The experiments on the demonstration plant showed a possible temperature difference,  $\Delta T_{\text{Reactor}}$ , in the single reactor vessels ranging from 1 to 3 K. The distillate output of each stage can be calculated using the following equation:

$$\dot{m}_{\text{dist}} = \frac{(\sum_{i=1}^n \dot{m}_i c_p \Delta T_{\text{Stage},i}) \cdot t}{h_v}$$

### 3.1. Evaporator modeling

It is necessary to model the evaporation and the condensation process separately for each stage. The reduction of each stage,  $i$  with one evaporator and one condenser can be seen in Fig. 4, which illustrates the previous stage  $i-1$  and the subsequent one  $i+1$ . Only the first stage has to be modeled differently because of the incoming saltwater flow after the heat supply in HEX1 [6].

Due to simplifications, the simulation neglects all heat and friction losses so that the spraying process can be assumed as steady flow with a constant enthalpy for all stages. This allows the formulation of

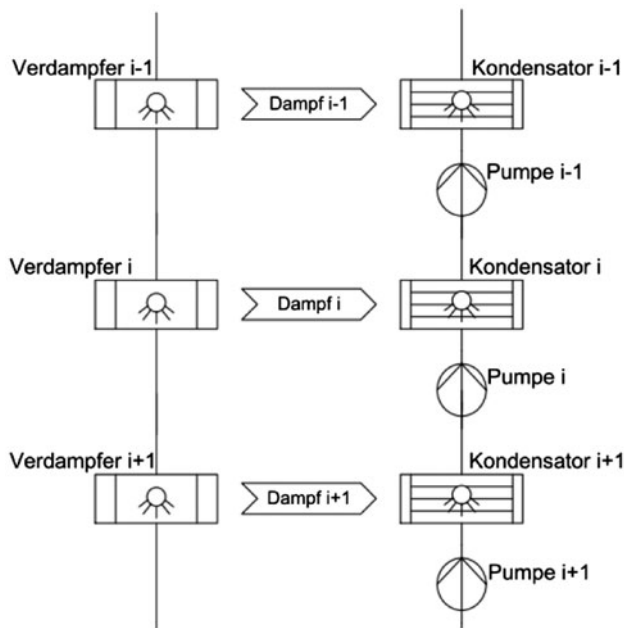


Fig. 4. Reduction of the model to stage  $i$  [6].

the following enthalpy balance, where as  $h_{\text{evap},i-1}$  is the specific enthalpy before the spraying and  $h_{\text{spray},i}$  after the spraying [6].

$$\frac{dU}{d\tau} = h_{\text{evap},i-1} - h_{\text{spray},i} = 0$$

The expansion during the spraying process lowers the pressure of the saltwater to the respective pressure of the reactor,  $i$  corresponding to the vapor pressure  $p_{\text{evap},i}$  calculated from the system temperatures  $T_{\text{evap},i}$  in the last section. The steam content  $x_{\text{evap},i}$  evolving from the saltwater in the evaporator increases and can be calculated by assuming  $h'$  as specific enthalpy of the boiling liquid and  $h''$  as saturated steam, respectively.

$$x_{\text{evap},i} = \frac{h'(T_{\text{evap},i-1}) - h'(T_{\text{evap},i})}{h''(T_{\text{evap},i}) - h'(T_{\text{evap},i})}$$

The salt content of the steam is assumed to be zero. The measurements on the demonstration plant have shown residual salt content lower than 30 ppm TDS [5]. The distillate mass flow  $\dot{m}_{\text{dist},i}$  after the first stage can be now approximated by this formula:

$$\dot{m}_{\text{dist},i} = x_{\text{evap},i} \cdot \dot{m}_{\text{evap},i-1}$$

The specific enthalpy of the distillate  $h_{\text{dist},i}$  corresponds to the state of saturated steam  $h''(T_{\text{evap},i})$ . Thus, the specific enthalpy of the salt water flowing in the subsequent reactor is assumed to have the enthalpy of boiling liquid  $h'(T_{\text{evap},i})$ . Having the mass flow of the distillate, it is now possible to calculate the mass flow entering the subsequent stage  $i+1$ . The process implies that after each stage, the salt concentration needs to increase which is given by the next formula [6].

$$\dot{m}_{\text{evap},i+1} = \dot{m}_{\text{evap},i} - \dot{m}_{\text{dist},i}$$

$$x_{\text{salt},i+1} = x_{\text{salt},i} \cdot \frac{\dot{m}_{\text{evap},i}}{\dot{m}_{\text{evap},i+1}}$$

This procedure allows the simulation of any desired amount of stages by the given salt water flows.

### 3.2. Condenser modeling

The condensation has to be modeled differently but can use all fluid properties, mass flows, and enthalpies calculated in the evaporator part. The most significant difference compared to the evaporator is

the simulation of the pumps and the required electrical work for pumping the distillate into the subsequent condenser. This is necessary because of the increasing pressure level in each reactor to allow the condensation of the evolved steam. The flow direction is reverse compared with the evaporation so that the interaction of evaporator and condenser can be seen like a big counterflow heat exchanger.

The simulation of the required pumping power is implemented by using enthalpy differences of each condenser stage under the assumption of an ideally isentropic compression of the distillate, excluding the first condenser stage. The pressure level corresponds to the evaporator stage  $i - 1$  calculated in the evaporator part by  $p_{\text{evap},i-1}$ . This allows the calculation of the ideal specific enthalpy of the pump  $h_{\text{pump,isen},i}$  in dependence of the specific entropy  $s_{\text{cond},i}$  and the pressure  $p_{\text{evap},i-1}$ , respectively. To calculate the real specific enthalpy, the isentropic efficiency ratio  $\eta_s$  is used [6].

$$h_{\text{pump,real},i} = (h_{\text{pump,isen},i} - h_{\text{cond},i+1}) \cdot \frac{1}{\eta_s} + h_{\text{cond},i+1}$$

The required pumping power can be derived using the mass flow and mechanical efficiency ratio  $\eta_m$  of the pump. Summing up all pumps between each condenser gives the total pumping power required in the condenser.

$$\dot{W}_{\text{pump},i} = (h_{\text{pump,real},i} - h_{\text{cond},i+1}) \cdot \dot{m}_{\text{cond},i+1} \cdot \frac{1}{\eta_m}$$

$$\dot{W}_{\text{pump,total}} = \sum_{i=1}^{n-1} \dot{W}_{\text{pump},i}$$

After pumping the distillate to the next condenser stage, it causes the condensation of the water vapor. This increases the mass flow and the temperature of the distillate by each condenser stage. The mass and entropy balance gives the added quantity and new fluid properties of the distillate similar to the evaporator part.

$$\dot{m}_{\text{cond},i} = \dot{m}_{\text{cond},i+1} + \dot{m}_{\text{dist},i}$$

$$h_{\text{cond},i} = (h_{\text{pump,real},i} \cdot \dot{m}_{\text{cond},i+1} + h_{\text{dist},i} \cdot \dot{m}_{\text{dist},i}) \cdot \frac{1}{\dot{m}_{\text{cond},i}}$$

So the thermodynamic state of the fluid at the exit of the reactor,  $i$  is defined and the specific entropy  $s_{\text{cond},i}$  can be calculated depending on  $h_{\text{cond},i}$  and  $p_{\text{cond},i}$  needed for the determination of the pumping power [6].

It is very important to avoid a phase change in the condenser reactors (boiling distillate) and to ensure that the distillate flow can easily take up all energy from the distillate steam, otherwise the simulation will be incorrect. Operational experience from the real demonstration plant shows that the pumps have problems with cavitation. All calculation results are visualized in Fig. 5, showing the LTD process overview and especially the conditions within a four-stage LTD system.

#### 4. CSP plant

A simplified process scheme with the solar libraries of Epsilon Professional [8] is used to simulate a direct-steam fresnel CSP system with 9.97 MW<sub>th</sub> effective solar heat. Epsilon allows the simulation of commercial-available concentrating solar thermal collectors with detailed data on geometry and performance. The calculation is performed using the data-set of the NOVATEC linear fresnel collector [9] with direct steam generation up to 460°C based on data for local conditions in El Gouna, Egypt. The steam turbine is modeled as two-stage system from Siemens (SST-110) with a high- and low-pressure part [10] expanding the generated steam from 60 to 0.4 bar, while reducing the temperature from 456 to 76°C. The steam mass flow is set to 12 t/h resulting in an electrical power generation of approx. 2.3 MW<sub>el</sub>. Fig. 6

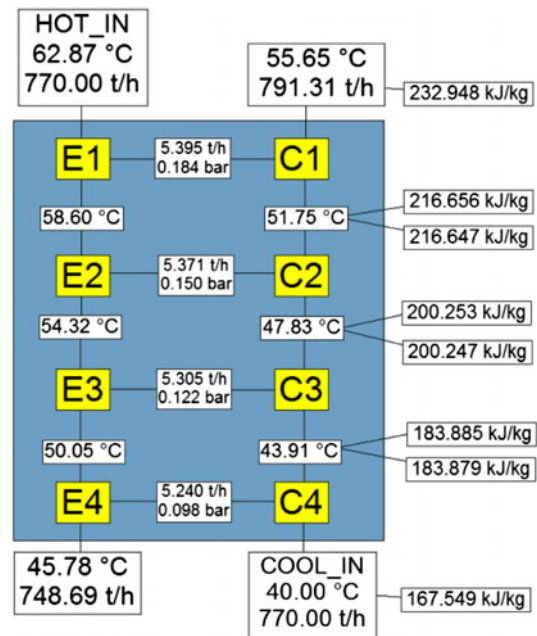


Fig. 5. LTD process overview for four stages.

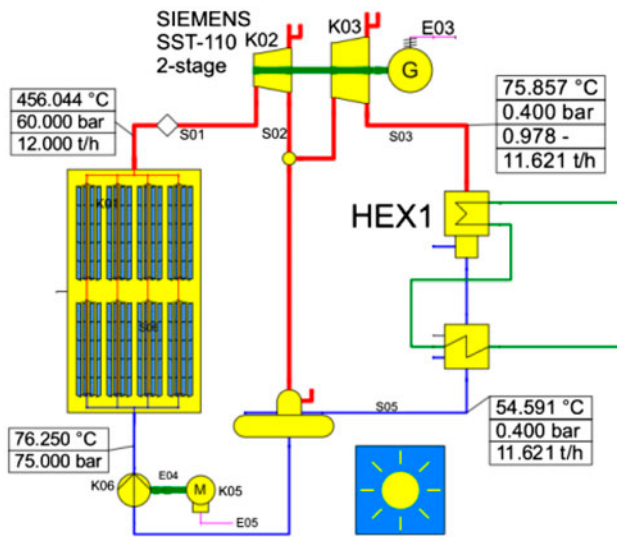


Fig. 6. CSP system with direct steam generation.

shows the designed simplified CSP system with feed-water pump, solar field, turbines, condenser, deaerator, and some process parameters. Blue lines indicate liquid water; red lines, steam; and green lines, a water/salt mixture.

The condensing temperature and pressure are determined by the mass flow and heat transfer to the

desalination system. Using the stated system, the turbine outlet pressure and its steam temperature can be lowered to 0.4 bar and 75°C. A lower turbine outlet pressure would allow higher electric power generation but less desalinated water. Anyway, the complete condensation of the steam needs to be ensured. To improve the heat extraction for the LTD system, an additional sub-cooler is modeled, which cools the CSP feed water down to 54°C. In a real system, this heat exchanger will be designed as one condenser with the properties to allow the sub-cooling needed. This transfers approx. 7.6 MW<sub>th</sub> heat to the desalination system.

### 5. Simulation results

The combination of the 10 MW<sub>th</sub> CSP system and the desalination can be now modeled. The heat exchanger 1 (HEX1) can be seen as interface between power generation and desalination. So the desalination system is supplied by the condensation heat of the steam in the power block. Fig. 7 shows the complete process in Epsilon Professional and some exemplary values.

The performance of this combined heat and power plant can be analyzed regarding electrical power generation, distillate production, heat input, and energy consumption. It could be shown that the main influences are the condensing steam pressure in HEX1

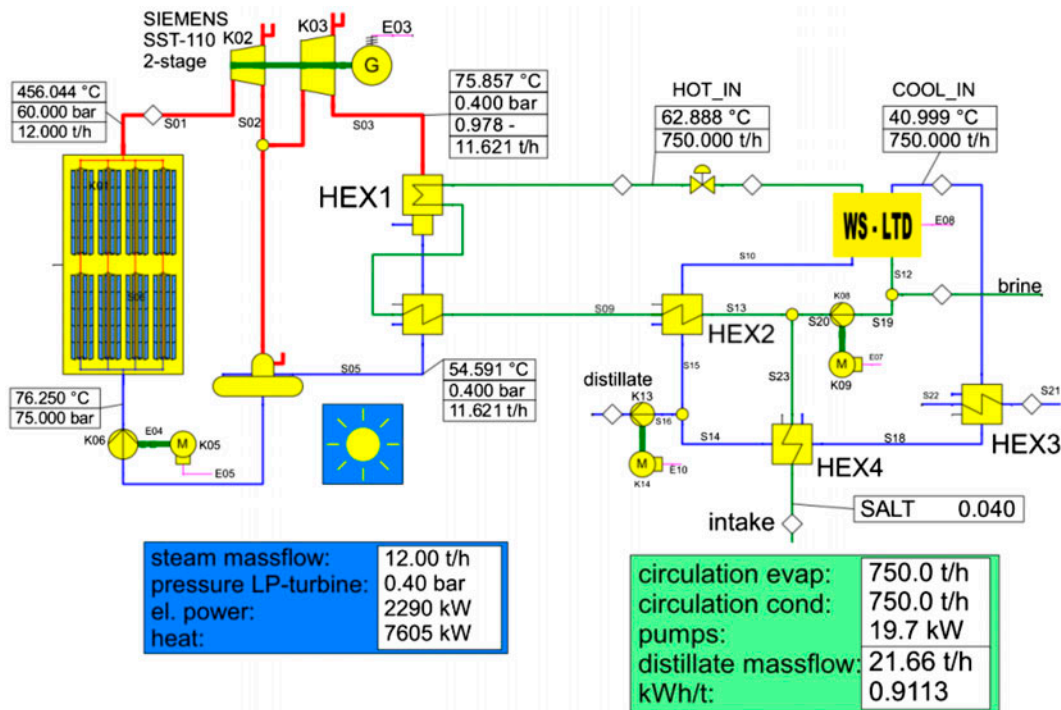


Fig. 7. Combination of CSP and desalination system.

of the CSP plant, the circulation mass flows of the desalination system, and the sea water salinity. Furthermore, increasing the number of stages improves the heat efficiency and water production of the desalination system, but also leads to higher the investment costs.

### 5.1. Start parameters

The most important initial parameters are listed in Table 1. It should be mentioned that the minimal temperature difference in HEX1, 2, and 4 is smaller compared with HEX3. This heat exchanger is intended to simulate a cooling cycle, which is not integrated in this simulation yet. The cooling mass flow is set to 1,500 m<sup>3</sup>/h to ensure sufficient heat removal in the desalination system. The efficiency ratios of the pumps and the motors are assumed to be ideal at 100% to

simplify the process. The salt content corresponds to the measured sea water salinity of the Red Sea in El Gouna, Egypt, and is set to 40 g/l TDS.

The power output of the solar field is subject to variations during the day. The simulation neglects this and calculates only the peak of the day in steady-state conditions. All location parameters are set to El Gouna, Egypt, with an approximated DNI of 900 W/m<sup>2</sup>. Actual measurements have shown values ranging from 600 to 1,100 W/m<sup>2</sup>.

### 5.2. Simulation results

It is important to change the parameters in a differentiated way for each simulation. For some more detailed analysis, it is necessary to modify selected parameters, which will be mentioned in the respective section. The main results are listed in the Table 2 below.

Table 1  
Simulation start parameter

Desalination system	Evaporator mass flow	750	m <sup>3</sup> /h
	Condenser mass flow	750	m <sup>3</sup> /h
	Number of stages	4	–
	Efficiency ratio (isentropic, mechanic)	100	%
	Salt content	40	g/l TDS
	Max. temperature Intake	62.9	°C
	Cooling temperature	40	°C
CSP system	Solar field size (60 collector units)	44,820	m <sup>2</sup>
	Location DNI, El Gouna, Egypt	900	W/m <sup>2</sup>
	Steam mass flow	12	t/h
	Steam pressure	60	bar
	Solar field pressure loss	15	bar
	Condensation pressure HEX1	0.4	bar

Table 2  
Simulation results

Desalination system	Distillate mass flow	21.66	m <sup>3</sup> /h
	Elec. power consumption for pumping	19.7	kW <sub>el</sub>
	Spec. power consumption	0.91	kWh/m <sup>3</sup>
	Spec. heat demand (4 stages)	1,291	kJ/kg
	Top brine temperature	58.7	°C
CSP system	Salinity brine	55	g/l TDS
	Solar field effective heat generation	9,974	kW <sub>th</sub>
	Solar field power generation	2,290	kW <sub>el</sub>
	Temperature before solar field	76.2	°C
	Pressure before solar field	75	bar
	Temperature after solar field	456	°C
	Pressure after solar field	60	bar
Condensation heat	7,605	kW <sub>th</sub>	

The results correspond with the measured values of the demonstration plant and with the given data of the manufacturers [5]. Nevertheless, it needs to be mentioned that some simplifications should have a negative impact on the distillate production and the specific power consumption, especially the efficiency ratios of the circulation pumps. But compared to conventional MED or MSF plants, the simulated LTD system is still more efficient and cost effective for the selected power range.

## 6. Discussion

In this section, some specific parameters are examined to investigate the behavior of the whole system. It turned out that the circulation mass flows in the desalination system used to run the spraying system in the reactors are especially important for the specific electrical power consumption and the overall efficiency of system [6].

### 6.1. Influence of the CSP condensation pressure

Fig. 8 shows the influence of the desalination system to the power generation in the CSP cycle without changes in the circulation mass flows. The condensation pressure directly corresponds to the maximal temperature entering the desalination system. Lowering this pressure increases the power generation but decreases the distillate production. Those simulation results are generated based on constant circulation mass flows. They need to be set to sufficiently high values so that mass flow allows the complete condensation of the steam in HEX1 after the low-pressure turbine. Thus, it can be seen that there is only a minor influence of the distillate production to the CSP power generation. This is due to the constant circulation mass flows having a negative impact on the specific power consumption of the desalination system.

### 6.2. Influence of the circulating mass flows

Fig. 9 illustrates the effect of minimized circulation mass flows ensuring a complete heat removal in HEX1 for the condensation in the CSP system. The CSP condensing pressure in HEX1 is varied from 0.18 to 0.7 bar with adapted mass flows to the temperature levels. Fig. 9 shows a significant increase in the distillate production due to decreased circulation mass flows and higher condensation pressures. This results in higher top brine temperatures and higher distillate production with decreasing specific energy consumption (less pumping power required). The specific

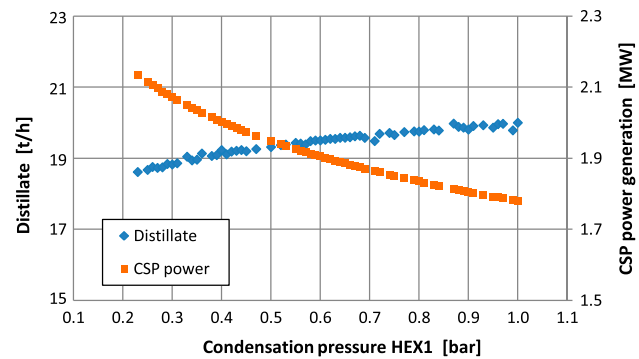


Fig. 8. Power generation depending on distillate production and condensation pressure [6].

power consumption and the distillate production are more or less constant at pressures above 0.5 bar. The opposite conclusion implies that for lowered condensation pressures, a higher mass flow is necessary due to the total system temperature gradient. So it can be concluded that the optimization of the mass flows has a major impact on the specific energy consumption and distillate production.

### 6.3. Influence of the number of stages

In Fig. 10, the number of stages is varied from 4 to 24. The figure shows a strong increase in the distillate production, while the specific energy consumption is slightly decreasing. The mass flows have been optimized to the respective number of stages in order to gain the maximum distillate output. Due to the system design, it is not necessary to double the circulation mass flows for each additional stage. It can be assumed that the optimal compromise between specific energy consumption, investment costs, and distillate production is reached with 14 stages.

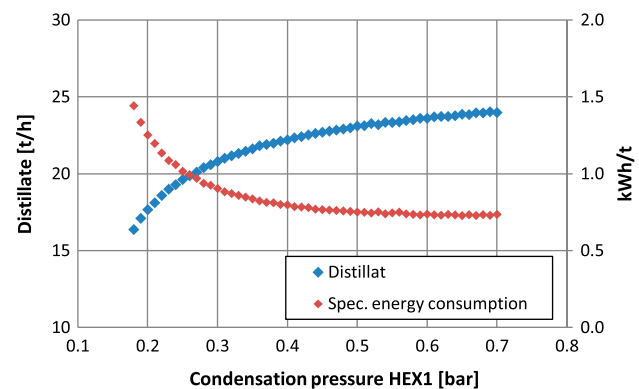


Fig. 9. Distillate production and specific power consumption with optimized mass flows [6].



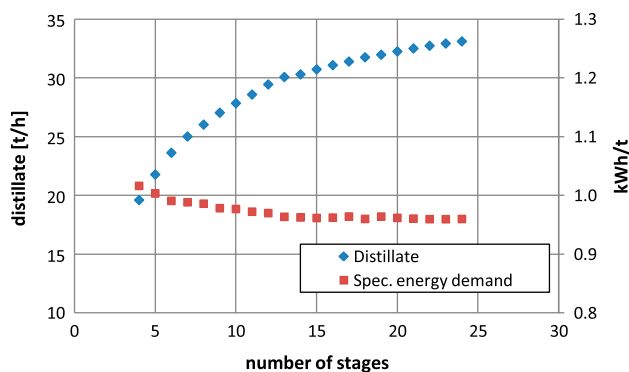


Fig. 10. Influence of the number of stages to distillate production [6].

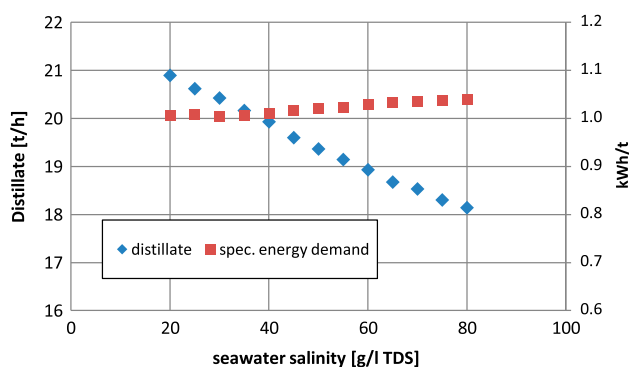


Fig. 11. Influence of the seawater salinity to distillate production [6].

#### 6.4. Influence of the seawater salinity

In Fig. 11, the influence of the seawater salinity is examined between values from 20 to 80 g/l TDS at four stages. The complete system is not prone to high feed water salt concentrations like every thermal desalination system. While the specific power consumption is pretty constant, the distillate production decreases with increasing feed water salt content. This is mainly due to the changed fluid properties of salt/water mixtures. There is a shift to higher evaporation temperatures on high concentrated solutions at constant pressures.

## 7. Conclusion

The combination of a CSP plant and a thermal seawater desalination plant has been modeled and the most important influence factors have been identified. The future research will focus on the optimization of the structure and the general plant concept with respect to the maximization of the power and water output and minimization of investment costs. This requires a more detailed CSP simulation with the

integration of a thermal storage system and an adapted cooling system for the selected location. However, balancing between sufficient heat transfers without lowering the power generation is one of the main challenges of this concept. This also requires careful dimensioning of the respective components. The next steps include a detailed exergy analysis to determine the efficiency of each component and an exergo-economic analysis to evaluate the plant's costs structure.

The reduction of the specific electricity consumption of the desalination system will also be part of the optimizations. There are several possible approaches for an optimized design of the reactors. The comparison with MED and MED-TVC systems [4] could show the advantages of this system due to no use of low-pressure motive steam for thermal vapor compression. The water production can be further increased using additional heat exchangers for preheating and suitable cooling systems. Another problem in terms of an appropriate brine treatment remains but could be solved with the conception of zero liquid discharge concepts for salt production.

## References

- [1] Water Risk Atlas, Aqueduct, World Resources Institute, 2012. Available from: <http://www.wri.org/our-work/project/aqueduct/aqueduct-atlas>.
- [2] F. Trieb, AQUA CSP Study, Concentrating Solar Power for Seawater Desalination, German Aerospace Center (DLR), Institute of Technical Thermodynamics, Section Systems Analysis and Technology Assessment, Stuttgart, 2007.
- [3] F. Trieb, H. Müller-Steinhagen, Concentrating solar power for seawater desalination in the Middle East and North Africa, German Aerospace Center, Institute of Technical Thermodynamics, Stuttgart, Germany, Desalination 220 (2008) 165–183.
- [4] M. Moser, F. Trieb, T. Fichter, Potential of concentrating solar power plants for the combined production of water and electricity in MENA countries, J. Sustain. Dev. Energy Water Environ. Syst. 1(2) (2013) 122–140, doi: <http://dx.doi.org/10.13044/j.sdewes.2013.01.0009>.
- [5] M. Lehmann, Low temperature distillation system by Watersolutions AG, General plant and process description, Watersolutions AG, Buchs, Switzerland, 2012.
- [6] K. Neuhäuser, Modellierung einer Niedertemperatur-Entsalzungsanlage mit Integration in ein solarthermisches Kraftwerk, Bachelorthesis, Institut für Energietechnik, TU Berlin, May 2013.
- [7] M. Lehmann, Process Comparison MED/LTD, Watersolutions AG, Buchs, Switzerland, 2013.
- [8] EBSILON<sup>®</sup>, Professional Documentation and Solar library, Version 10.0, Build: 10.0.0.16731, February, 2012
- [9] Novatec Linear Fresnel collector, implemented in Ebsilon solar library, February 2012.
- [10] Siemens Turbomachinery Equipment GmbH, Cornelia Liebmann, Budget-Offer 127243-1A from 02.05.2012, Two-stage Steam Turbine SST-110.